

Modeling and Analysis of DC-DC SEPIC Converter with Coupled Inductors

Onur KIRCIOĞLU

Electrical Engineering Department
Kocaeli University
Kocaeli, Turkey
onur.kircioglu@kocaeli.edu.tr

Murat ÜNLÜ

Electrical Engineering Department
Kocaeli University
Kocaeli, Turkey
muratunlu@kocaeli.edu.tr

Sabri ÇAMUR

Electrical Engineering Department
Kocaeli University
Kocaeli, Turkey
scamur@kocaeli.edu.tr

Abstract— Nowadays, DC/DC converters are widely used in industrial applications and renewable energy systems. A SEPIC (single-ended primary inductance converter) DC-DC converter is capable of operating in either step-up or step-down mode and commonly used in a battery charger system. This paper presents the modeling and analyzing of the SEPIC with coupled and uncoupled inductors. In this study, the state-space averaged (SSA) model is established and built in MATLAB/Simulink environment. The obtained SEPIC model was simulated for different input parameters, and results of coupled and uncoupled are compared. Moreover, the small signal model is used for linearization of the SSA model of the SEPIC with coupled and uncoupled inductors, hence the transfer function of control (duty cycle) to output voltage is formulated. Bode plots of the duty cycle to output voltage transfer functions are constructed, and the result can be used in various applications to design a closed-loop controller to regulate the output voltage.

Keywords— DC/DC SEPIC converter, State-space averaged model, small signal model, transfer function.

I. INTRODUCTION

The switching mode DC/DC converters can be realized by different circuit topologies. Among them the buck, boost, buck-boost, Cuk, and SEPIC (Single-Ended Primary Inductor Converter) converters are the mostly used depends on requirements for power conversion system. It has become popular in recent years step up or down DC-DC converters are useful in applications where the battery voltage can be above or below the regulator output voltage. The converter must be able to operate as step up or down in order to continue supplying the constant load voltage over the entire battery voltage range [1].

Each of these converters has its advantages and disadvantages. The SEPIC is not the finest as an efficiency and cost among these converters [2]. But it possesses several significant advantages with regard to the other converters. The other advantages could be summarized as follows:

- SEPIC is able to generate output voltage greater than, less than, or equal to the input voltage
- having non-inverting output
- easy-to drive switch because the switch referenced to the ground node

- low input-current pulsating, it is desirable and important to precisely track maximum power point application for photovoltaic systems and to reduce EMI, and thus reduce the necessity for additional filter elements

The SEPIC converter has four energy storage elements (two capacitors, two inductors). Therefore, four state –variables occur, and it makes the converter a fourth order non-linear system, and hence modeling the converter is rather difficult issue.

In literature, SEPIC DC/DC converter is frequently used in photovoltaic energy system with a maximum power point tracking and also as a battery charger [2-7]. Furthermore, it is utilized in power factor correction applications and LED drivers [8-12]. In [2], a SEPIC converter modeling and control was realized for battery charger system. Besides, detailed comparison of various buck-boost converters are given in this study. In [1], State-Space Averaging (SSA) technique was used in order to obtain transfer function of SEPIC with uncoupled inductor presents modeling of a SEPIC converter operating in Continuous Conduction Mode (CCM).

In this paper, firstly, SEPIC converter circuit topologies for two switching modes are presented, Secondly, steady-state model, dynamic model and transfer functions of SEPIC with coupled inductor are obtained via state-space averaging and small signal methods in CCM mode. After dynamic model a SEPIC converter is built, SEPIC with uncoupled and coupled inductors is analyzed for different parameters and compared each other's. In third stage, the bode diagrams of SEPIC with coupled inductor and uncoupled inductor are given. These results can be used in order to design a controller, like definition of parameters of PID control.

II. SEPIC CONVERTER TOPOLOGY

The SEPIC converter is consists of an active power switch (MOSFET), a diode, two inductors (L_1 , L_2) and two capacitors (C_1 , C_2) shown in Fig. 1. C_1 capacitor, which is between the inductors L_1 and L_2 , ensure DC isolation which blocks any DC current path between the input and the output [9]. If the SEPIC converter is operating in the CCM, two switching modes are considered and the equivalent circuits belong to each mode are given in Fig.2. In Mode 1 (S_1 is turned on) L_1 and L_2 are charged by V_i and V_{C1} , respectively as depict in Fig.2a. In Mode 2, (S_1 is turned off) C_1 and C_2 are discharged by i_{L2}

and the output current as depict in Fig.2b. The inductors L1 and L2 can be used uncoupled, which are separated or coupled which are wound on the same core. This paper investigates behavior of SEPIC and presents results obtained from simulation for both situations.

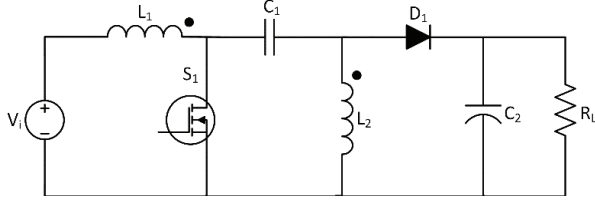


Fig. 1. The equivalent circuit of SEPIC converter

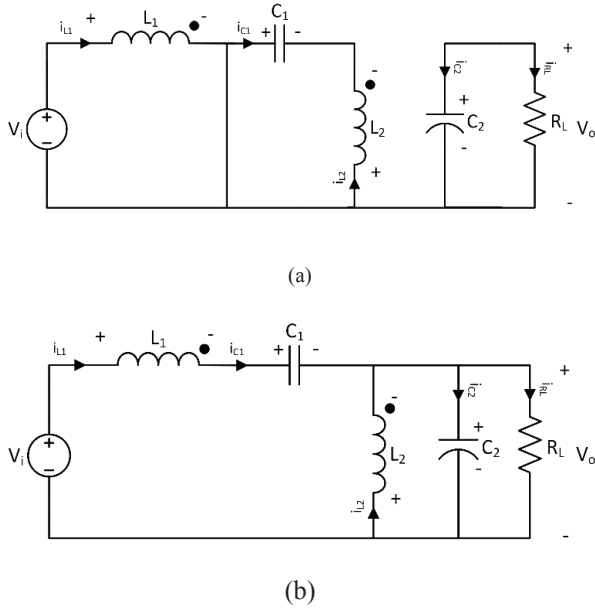


Fig. 2. The equivalent circuit of SEPIC converter in (a) Mode 1 (S1 is on) (b) Mode 2 (S1 is off)

III. STATE SPACE AVARAGED MODEL OF COUPLED INDUCTOR SEPIC CONVERTER

A modeling for SEPIC converter is required in order to analyze the SEPIC behavior and design its corresponding controllers. The state-space averaged model is widely used as a mathematical model for the converter control design. The state-space averaged method derives an equivalent model in matrix forms by averaging all the system variables in a switching period. By placing the matrices into the final equations give the steady-state model, dynamic model and transfer functions of the converter. Meanwhile, the switching frequency is fairly greater than the natural frequency of system variables and the converter operates in CCM mode are assumed. Besides, ESR (the equivalent series resistance) and ESL (the equivalent series inductance) of capacitances (C1 and C2) are neglected, and the ESRs of two inductances (L1 and L2) are ignored. It is widely known that state-space equations of any system can be represented as in (1). The state equations of SEPIC with

coupled inductor for Mode 1 and Mode 2 situations are given in (2) and (3), respectively, and illustrated in Fig.2

$$[\dot{X}] = [A][X] + [B][U] \quad (1)$$

Mode 1: State-Space Equation with the state variables to find their respective derivatives set in Mode 1 as follows (2):

$$\left. \begin{aligned} L_1 \frac{di_{L1}}{dt} + M \frac{di_{L2}}{dt} &= V_i \\ L_2 \frac{di_{L2}}{dt} + M \frac{di_{L1}}{dt} &= V_{C1} \\ C_1 \frac{dv_{C1}}{dt} &= -i_{L2} \\ C_2 \frac{dv_{C2}}{dt} &= \frac{-V_{C2}}{R_L} \end{aligned} \right\} \quad (2)$$

Mode 2: State-Space Equation with the state variables to find their respective derivatives set in Mode 2 as follows (3):

$$\left. \begin{aligned} L_1 \frac{di_{L1}}{dt} + M \frac{di_{L2}}{dt} &= V_i - V_{C1} - V_{C2} \\ L_2 \frac{di_{L2}}{dt} + M \frac{di_{L1}}{dt} &= -V_{C2} \\ C_1 \frac{dv_{C1}}{dt} &= i_{L1} \\ C_2 \frac{dv_{C2}}{dt} &= i_{L1} + i_{L2} - \frac{V_{C2}}{R_L} \end{aligned} \right\} \quad (3)$$

The state-space models of SEPIC with coupled inductor for Mode1 and Mode 2 are given in (4) and (5), separately. The state space averaged model in CCM is obtained by averaging the state space matrices of the Mode 1 and Mode 2 over a period. By defining the duty cycle "D", the state space averaged model of the SEPIC with coupled is obtained as (8) with F matrix. There, M stands for mutual inductance and it is zero for uncoupled inductor. To obtained singly A and B matrices, the equation given in (10) must be used.

$$\underbrace{\begin{bmatrix} L_1 & M & 0 & 0 \\ M & L_2 & 0 & 0 \\ 0 & 0 & C_1 & 0 \\ 0 & 0 & 0 & C_2 \end{bmatrix}}_{[F]} \underbrace{\begin{bmatrix} i_{L1} \\ i_{L2} \\ v_{C1} \\ v_{C2} \end{bmatrix}}_{[X]} = \underbrace{\begin{bmatrix} 0 & 0 & 0 & 0 \\ 0 & 0 & 1 & 0 \\ 0 & -1 & 0 & 0 \\ 0 & 0 & 0 & -1/(R_L) \end{bmatrix}}_{[A_1']} \underbrace{\begin{bmatrix} i_{L1} \\ i_{L2} \\ v_{C1} \\ v_{C2} \end{bmatrix}}_{[X]} + \underbrace{\begin{bmatrix} 1 \\ 0 \\ 0 \\ 0 \end{bmatrix}}_{[B_1']} [V_i] \quad (4)$$

$$\underbrace{\begin{bmatrix} L_1 & M & 0 & 0 \\ M & L_2 & 0 & 0 \\ 0 & 0 & C_1 & 0 \\ 0 & 0 & 0 & C_2 \end{bmatrix}}_{[F]} \underbrace{\begin{bmatrix} i_{L1} \\ i_{L2} \\ v_{C1} \\ v_{C2} \end{bmatrix}}_{[X]} = \underbrace{\begin{bmatrix} 0 & 0 & -1 & -1 \\ 0 & 0 & 0 & -1 \\ 1 & 0 & 0 & 0 \\ 1 & 1 & 0 & -1/(R_L) \end{bmatrix}}_{[A_2']} \underbrace{\begin{bmatrix} i_{L1} \\ i_{L2} \\ v_{C1} \\ v_{C2} \end{bmatrix}}_{[X]} + \underbrace{\begin{bmatrix} 1 \\ 0 \\ 0 \\ 0 \end{bmatrix}}_{[B_2']} [V_i] \quad (5)$$

$$[A] = [A_1]D + [A_2](1 - D) \quad (6)$$

$$[B] = [B_1]D + [B_2](1 - D) \quad (7)$$

$$\underbrace{\begin{bmatrix} L_1 & M & 0 & 0 \\ M & L_2 & 0 & 0 \\ 0 & 0 & C_1 & 0 \\ 0 & 0 & 0 & C_2 \end{bmatrix}}_{[F]} \begin{bmatrix} \dot{i}_{L_1} \\ \dot{i}_{L_2} \\ \dot{v}_{C_1} \\ \dot{v}_{C_2} \end{bmatrix} = \underbrace{\begin{bmatrix} 0 & 0 & (D-1) & (D-1) \\ 0 & 0 & D & (D-1) \\ (1-D) & -D & 0 & 0 \\ (1-D) & (1-D) & 0 & -1/(R_L) \end{bmatrix}}_{[A']} \begin{bmatrix} i_{L_1} \\ i_{L_2} \\ v_{C_1} \\ v_{C_2} \end{bmatrix} + \underbrace{\begin{bmatrix} 1 \\ 0 \\ 0 \\ 0 \end{bmatrix}}_{[B']} [V_i] \quad (8)$$

$$[A_1] = [F]^{-1}[A_1'], \quad [B_1] = [F]^{-1}[B_1'], \quad [A_2] = [F]^{-1}[A_2'], \\ [B_2] = [F]^{-1}[B_2'],$$

$$[A] = [F]^{-1}[A'], \quad [B] = [F]^{-1}[B'] \quad (10)$$

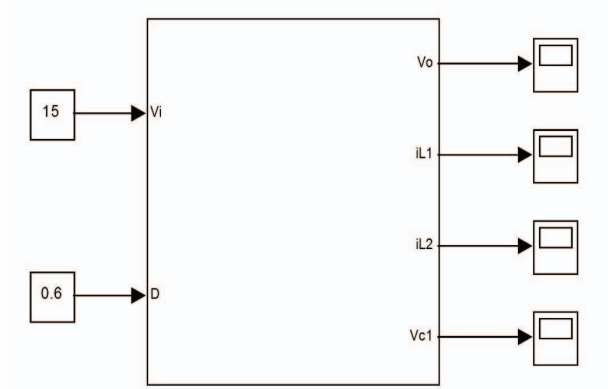


Fig. 3. The SEPIC converter SSA model built in MATLAB/Simulink

In simulation studies, the following parameters for the SEPIC converter are chosen: L_1 and L_2 are 340 μH , $C_1 = 20 \mu\text{F}$, $C_2 = 680 \mu\text{F}$, $R_L = 5 \Omega$, $V_i = 20 \text{ V}$. The switching frequency is 100 kHz. Since SEPIC converters can operate as a step up or step down, V_o output voltage 30 V and 13.3 V are selected, respectively. In this study, coupling factor, k is selected 0.98, hence Mutual inductance, M is calculated as 333.2 μH . The simulation results related to output voltage of SEPIC with coupled inductor for two different duty cycle (D) are given in Fig. 4, Fig.5, and Fig.6. In addition, the waveform of the input currents or L_1 inductor currents i_{L1} for coupled inductors and uncoupled inductors are illustrated in Fig. 7 and Fig. 9, respectively. Fig. 8 shows the waveform of L_2 inductor currents i_{L2} related to SEPIC with coupled inductors.

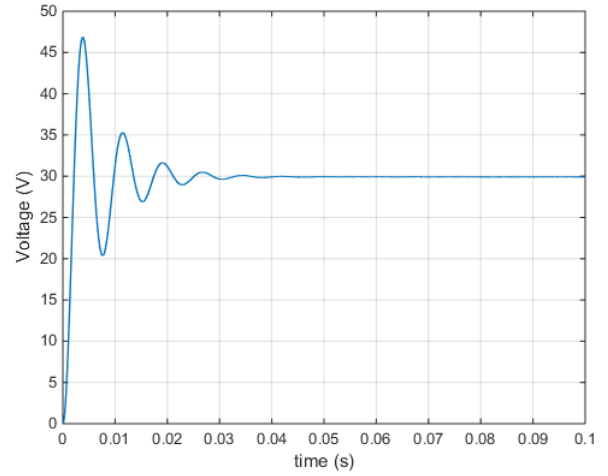


Fig. 4. Output Voltage of the converter ($D=0.6$)

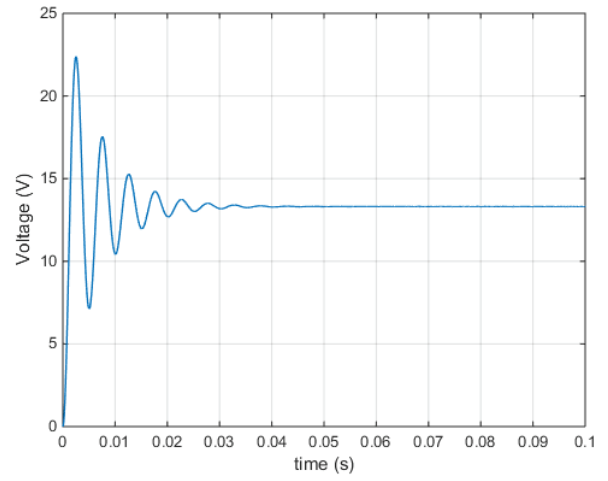


Fig. 5. Output voltage of the converter ($D=0.4$)

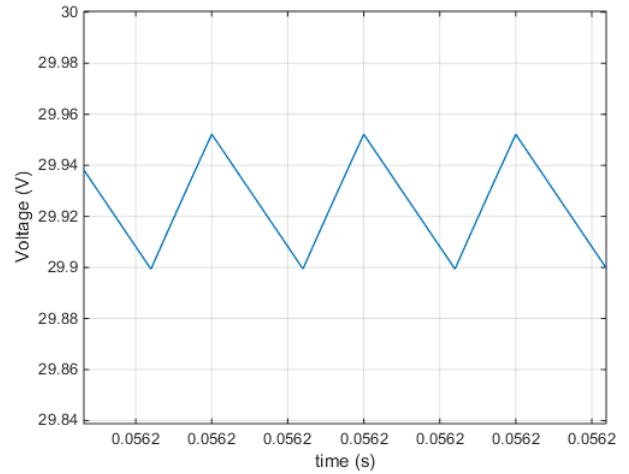


Fig. 6. Closer look at the output voltage ($D=0.6$)

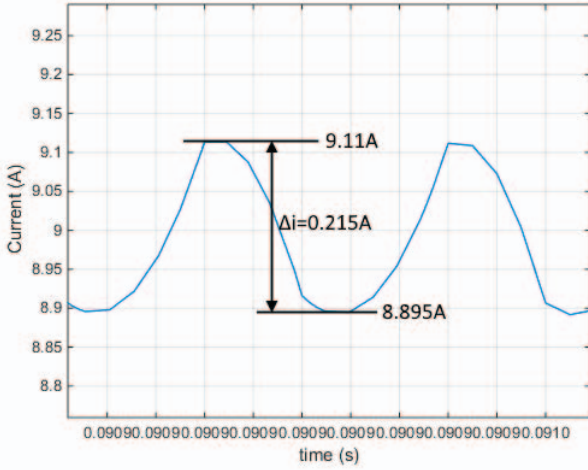


Fig. 7. Waveform of the input current (i_{L1}) for L_1 coupled inductor situation

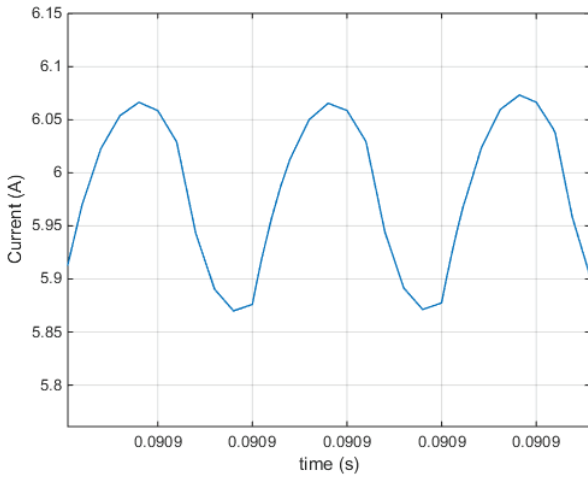


Fig. 8. Waveform of the L_2 current (i_{L2})

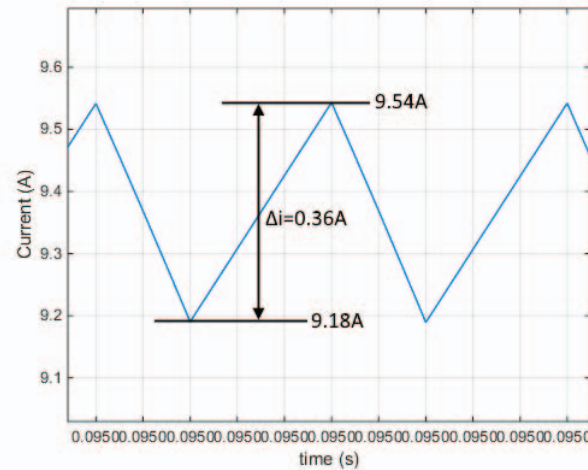


Fig. 9. Waveform of the input current (i_{L1}) for L_1 uncoupled inductor situation

IV. SMALL SIGNAL ANALYSIS OF COUPLED INDUCTOR SEPIC CONVERTER

The small signal model of the converter is then derived by linearizing the state-space averaging model around an operating point. It is used to derive all the desired transfer functions of converter to design a linear control system by using classical control techniques.

To obtain small signal model of system, the variables are perturbed around a steady-state operating point are assumed as given in (11), where X , D , U and Y represent steady-state values, \hat{x} , \hat{d} , \hat{u} , and \hat{y} represent small-signal values.

$$\begin{cases} x = X + \hat{x} \\ d = D + \hat{d} \\ u = U + \hat{u} \\ y = Y + \hat{y} \end{cases} \quad (11)$$

$$X = -A^{-1}BU$$

$$Y = -c^T A^{-1}BU$$

$$\begin{aligned} \dot{\hat{x}} = & x[A_1(D + \hat{d}) + A_2(1 - D - \hat{d})](X + \hat{x}) \\ & + [(B_1(D + \hat{d}) + B_2(1 - D - \hat{d}))](V_i + \hat{u}) \end{aligned}$$

$$\hat{y} = c_1^T(X + \hat{x})(D + \hat{d}) + c_2^T(X + \hat{x})(1 - D - \hat{d})$$

$$\hat{x} = A\hat{x} + B\hat{u} + [(A_1 - A_2)X + (B_1 - B_2)U]\hat{d}$$

$$\hat{y} = c^T\hat{x} + (c_1^T - c_2^T)X\hat{d}$$

The Laplace transfer function of the converter can be derived as in (12), transfer function is;

$$\begin{aligned} s\tilde{x}(s) = & A\tilde{x}(s) + B\tilde{v}_i(s) + \\ & [(A_1 - A_2)X + (B_1 - B_2)V_i]\tilde{d}(s) \end{aligned} \quad (12)$$

By rearranging (12), (13) is obtained, where I represents the identity matrix.

$$[sI - A]\tilde{x}(s) = B\tilde{v}_i(s) + [(A_1 - A_2)X + (B_1 - B_2)V_i]\tilde{d}(s) \quad (13)$$

$$\tilde{y} = \tilde{v}_o(s) = c^T\tilde{x}(s) \quad (14)$$

Equation (14) is used to get output voltage, and finally from (15), the transfer function of control to output voltage of is attained as in (16). The bode plots of the transfer function of SEPIC converter with coupled inductor and uncoupled inductor are drawn and illustrated in Fig. 10 and Fig. 11, respectively.

$$\frac{\tilde{v}_o(s)}{\tilde{d}(s)} = [0 \ 0 \ 0 \ 1][sI - A]^{-1}[(A_1 - A_2)X + (B_1 - B_2)V_i] \quad (15)$$

$$\frac{\tilde{v}_o(s)}{\tilde{d}(s)} = \frac{a_3s^3 + a_2s^2 + a_1s + a_0}{b_4s^4 + b_3s^3 + b_2s^2 + b_1s + b_0} \quad (16)$$

$$a_3 = C_1D(M^2 - L_1L_2)$$

$$\begin{aligned}
a_2 &= C_1 R_L (L_1 + L_2 - 2M - 2DL_1 - 2DL_2 + 4DM) + C_1 D^2 R_L (L_1 \\
&\quad + L_2 - 2M) \\
a_1 &= D^2 M - D^2 L_1 - DM \\
a_0 &= (1 - D)^2 R_L \\
b_4 &= C_1 C_2 R_L (L_1 L_2 - M^2) \\
b_3 &= C_1 (L_1 L_2 - M^2) \\
b_2 &= C_1 R_L (L_1 + L_2 - 2M - 2DL_1 - 2DL_2 + 4DM) \\
&\quad + C_2 R_L (L_2 - 2DL_2 + 2DM) + (C_1 D^2 R_L + C_2 D^2 R_L) (L_1 + L_2 - 2M) \\
b_1 &= L_2 - 2DL_2 + 2DM + D^2 (L_1 + L_2 - 2M) \\
b_0 &= (1 - D)^2 R_L
\end{aligned}$$

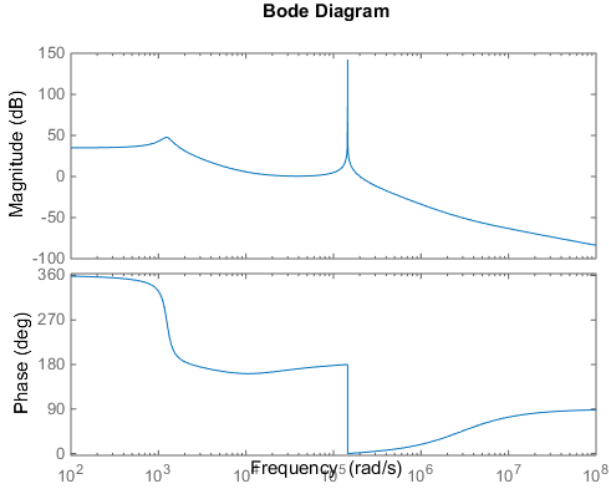


Fig. 10. Bode plot of the control to output transfer function of SEPIC with coupled inductor

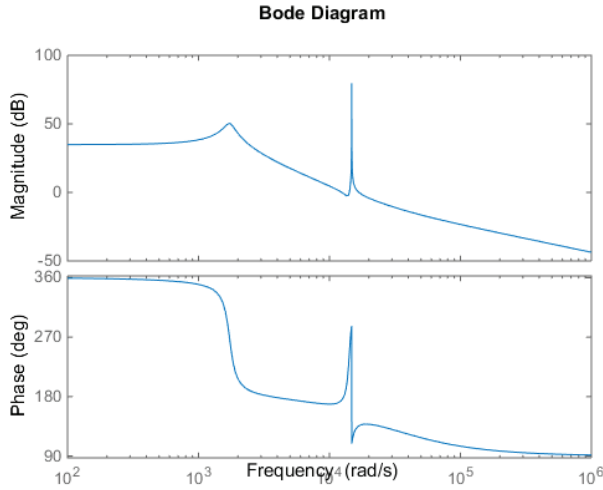


Fig. 11. Bode plot of the control to output transfer function of SEPIC with uncoupled inductor

V. CONCLUSION AND FUTURE WORKS

In this paper, the state space averaged method of SEPIC converter with coupled inductor is obtained. The model also can be used uncoupled inductor by changing the value of the mutual inductance ($M=0$). The obtained SSA method is simulated for different input parameters. It is observed from Fig. 7 and Fig. 9 that the input current ripple of the SEPIC with coupled is remarkably smaller than the input current ripple of uncoupled inductor. Thus, input current ripple could be reduced by using coupled inductor. It can be explained another way that providing the same ripple current with smaller inductance compared to uncoupled inductors. Afterward, the small signal linearization technique was applied to SSA in order to obtain control to output transfer function. The bode plots of control to output voltage transfer function are drawn for SEPIC with coupled and uncoupled inductor, respectively. And the results from Fig.10 and Fig.11 can be used in order to design a controller system for SEPIC converter.

REFERENCES

- [1] V. Eng and C. Bunlaksananusorn, "Modeling of a SEPIC converter operating in continuous conduction mode," in *Proc. 6th ECTI-CON*, May 2009, pp. 136–139.
- [2] S.J. Chiang et al., "Modeling and Control of PV Charger System With SEPIC Converter", *IEEE Trans. Ind. Electron.*, vol. 56, no. 11, pp. 4344–4353, Nov. 2009.
- [3] H.S. Chung et al., "Novel Maximum Power Point Tracking Technique for Solar Panels Using a SEPIC or Cuk Converter", *IEEE Trans. Power Electron.*, vol. 18, no. 3, pp. 717–724, May. 2003.
- [4] A.E. Khateb et al., "Maximum power point tracking of single-ended primary-inductor converter employing a novel optimisation technique for proportional-integral derivative controller", *IET Power Electron.*, Vol. 6, Iss. 6, pp. 1111–1121, 2013.
- [5] E.Mamarelis et al., "Design of a Sliding-Mode-Controlled SEPIC for PV MPPT Applications", *IEEE Trans. Ind. Electron.*, vol. 61, no. 7, pp. 3387–3398, Jul. 2014.
- [6] C. Cabal et al., "Maximum power point tracking based on sliding mode control for output-series connected converters in photovoltaic systems", *IET Power Electron.*, Vol. 7, Iss. 4, pp. 914–923, 2014.
- [7] M. Killi and S. Samanta, "An Adaptive Voltage-Sensor-Based MPPT for Photovoltaic Systems With SEPIC Converter Including Steady-State and Drift Analysis", *IEEE Trans. Ind. Electron.*, vol. 62, no. 12, pp. 7609–7619, Dec. 2015.
- [8] K.S Tey and S. Mekhilef, "Modified Incremental Conductance Algorithm for Photovoltaic System Under Partial Shading Conditions and Load Variation", *IEEE Trans. Ind. Electron.*, vol. 61, no. 10, pp. 5384–5392, Oct. 2014.
- [9] H.J. Chiu et al., "A High Efficiency Dimmable LED Driver for Low-Power Lighting Applications", *IEEE Trans. Ind. Electron.*, vol. 57, no. 2, pp. 735–743, Feb. 2010.
- [10] M. Mahdavi and H. Farzanehfard, "Bridgeless SEPIC PFC Rectifier With Reduced Components and Conduction Losses", *IEEE Trans. Ind. Electron.*, vol. 58, no. 9, pp. 4153–4160, Sept. 2011.
- [11] H. Ma et al., "A Novel Valley-Fill SEPIC-derived Power Supply Without Electrolytic Capacitors for LED Lighting Application", *IEEE Trans. Power Electron.*, vol. 27, no. 6, pp. 3057–3071, Jun. 2012.
- [12] M. Bodelto et al., "Design of AC–DC PFC High-Order Converters With Regulated Output Current for Low-Power Applications", *IEEE Trans. Power Electron.*, vol. 31, no. 3, pp. 2012–2025, Mar. 2016.